Secondary Fill Minimizes Gutter Size in Chimney EVAS Configurations In Vitro

Theodorus G. van Schaik, MD[1]*⬤, Jorn P. Meekel, MD[1]*,
Vincent Jongkind, MD, PhD[3], Rutger J. Lely, MD[2], Maarten Truijers, MD, PhD[1],
Arjan W. J. Hoksbergen, MD, PhD[1], Willem Wisselink, MD, PhD[1],
Jan D. Blankensteijn, MD, PhD[1], and Kak Khee Yeung, MD, PhD[1]

Abstract

Purpose: To investigate in an in vitro model if secondary endobag filling can reduce gutter size during chimney endovascular aneurysm sealing (chEVAS). **Materials and Methods:** Nellix EVAS systems were deployed in 2 silicone juxtarenal aneurysm models with suprarenal aortic diameters of 19 and 24 mm. Four configurations were tested: EVAS with 6-mm balloon-expandable (BE) or self-expanding (SE) chimney grafts (CGs) in the renal branches of both models. Balloons were inflated simultaneously in the CGs and main endografts during primary and secondary endobag filling and polymer curing. Computed tomography (CT) was performed immediately after the primary and secondary fills. Cross-sectional lumen areas were measured on the CT images to calculate gutter volumes and percent change. CG compression was calculated as the reduction in lumen surface area measured perpendicular to the central lumen line. The largest gutter volume and highest compression were presented per CG configuration per model. **Results:** Secondary endobag filling reduced the largest gutter volumes from 99.4 to 73.1 mm^3 (13.2% change) and 84.2 to 72.0 mm^3 (27.6% change) in the BECG configurations and from 67.2 to 44.0 mm^3 (34.5% change) and 92.7 to 82.3 mm^3 (11.2% change) in the SECG configurations in the 19- and 24-mm models, respectively. Secondary endobag filling increased CG compression in 6 of 8 configurations. BECG compression changed by −0.2% and 5.4% and by −1.0% and 0.4% in the 19- and 24-mm models, respectively. SECG compression changed by 10.2% and 16.0% and by 7.2% and 7.3% in the 19- and 24-mm models, respectively. **Conclusion:** Secondary endobag filling reduced paragraft gutters; however, this technique did not obliterate them. Increased CG compression and prolonged renal ischemia time should be considered if secondary endobag filling is used.

Keywords

aneurysm model, angulation, balloon-expandable stent-graft, chimney graft, compression, endobag, endograft, endoleak, endovascular aneurysm sealing, gutter, in vitro model, juxtarenal aneurysm, lumen area, lumen volume, self-expanding stent-graft, stent-graft

Introduction

In approximately 15% of abdominal aortic aneurysms (AAAs) there is no proximal seal zone below the renal arteries, precluding standard endovascular aneurysm repair (EVAR).[1] Open repair is considered the gold standard for juxtarenal aortic aneurysms but is associated with considerable mortality and morbidity.[2] Over the past decade, several endovascular techniques have been developed to treat juxtarenal aneurysms, such as customized fenestrated EVAR. The high costs and time required to produce a fenestrated endograft are major disadvantages of this technique. Combining off-the-shelf aortic stent-grafts with chimney grafts (CGs) may be a more cost-effective solution to treat this pathology.[3,4]

For endovascular repair with CGs, bilateral stent-grafts are deployed in the renal arteries and aligned parallel to the

[1]Department of Vascular Surgery, VU University Medical Center, Amsterdam, the Netherlands
[2]Department of Interventional Radiology, VU University Medical Center, Amsterdam, the Netherlands
[3]Department of Surgery, Westfriesgasthuis, Hoorn, the Netherlands

*Theodorus G. van Schaik and Jorn P. Meekel contributed equally to this work and have shared first authorship.

Corresponding Author:
Kak K. Yeung, Departments of Surgery and Physiology, VU University Medical Center Amsterdam, De Boelelaan 1118, 1081 HV Amsterdam, the Netherlands.
Emails: k.yeung@vumc.nl

main endograft. This technique extends the sealing zone of the main device to the healthy aortic wall proximal to the renal arteries while maintaining perfusion of the kidneys. A major asset of the chimney technique is the direct availability of off-the-shelf stent-grafts in case of very large, symptomatic, or ruptured aneurysms.[4] However, a common problem with CG configurations is a type Ia endoleak through so-called paragraft gutters. These leaks, which are observed in 11.5% to 18.0% of the cases, might cause aneurysm growth and eventual rupture.[4–7]

Several techniques to reduce or obliterate these gutters have been studied in vitro.[8–10] The Nellix EndoVascular Aneurysm Sealing (EVAS) system (Endologix, Irvine, CA, USA) is hypothesized to increase sealing between the endograft, CG, and aortic wall, thereby reducing gutter size.[11,12] The EVAS system consists of 2 parallel aortic endografts surrounded by endobags. Filling the endobags with polymer increases fixation and sealing in the entire aneurysm while simultaneously reducing paragraft gutters. After infusion, the polymer cures to form a biostable solution.[11,12] Nevertheless, complete eradication of these gutters was not demonstrated by earlier studies, so the use of EVAS does not rule out type Ia endoleaks. A probable cause may be incomplete enclosure of the CG by the endobag.

The Nellix system allows a secondary fill with a relatively small volume of polymer after the primary fill has cured to increase endobag apposition to the aortic wall. This secondary fill might reduce paragraft gutters, but there is not much literature available on the use of secondary fill in clinical practice. Brownrigg et al[13] indicated that they routinely perform secondary fill in case of low endobag pressures or sealing failure, and Gossetti et al[14] reported that 5% of their 335 patients underwent secondary fill during EVAS. However, the potential benefit of secondary fill is still unclear. The present study examined the impact of a secondary fill after polymer curing on paragraft gutter volumes after chimney EVAS (chEVAS) in juxtarenal aneurysm models.

Materials and Methods

Experimental Setup

Two silicone models (DBC Laboratories, Wheat Ridge, CO, USA) of a juxtarenal aortic aneurysm with suprarenal wall compliance mimicking the healthy human aorta (~5%) were used (Figure 1). The models were similar to ones used in previous studies investigating paragraft gutters.[10] They contained a distal bifurcation and 2 proximal side branches representing the renal arteries, which originated at the same 3 and 9 o'clock positions with a takeoff angle of 90°. There was no distance between the lower margin of the renal branch and the aneurysm. Both models had a nondilated suprarenal aorta with a length of 120 mm. Model I had a
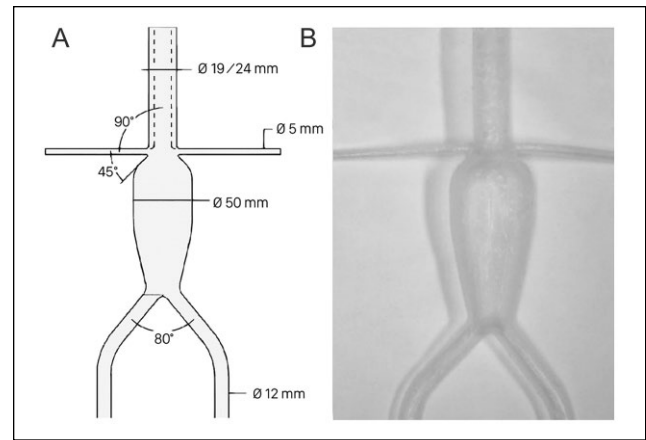

Figure 1. The juxtarenal aortic aneurysm models used for the chimney endovascular aneurysm sealing configurations. (A) The flow lumen measurements of the silicone models; diameters are presented in millimeters and angles in degrees. The dotted line represents the narrow suprarenal aortic aneurysm wall of the 19-mm model. (B) An image of the silicone model prior to the experiments.

suprarenal aortic diameter of 19 mm and model II had a suprarenal aortic diameter of 24 mm. The models were submerged in a gelatin-water solution (Sigma Chemical Corporation, St Louis, MO, USA) with viscosity similar to human blood, preventing air from entering the model.[15,16] The temperature was maintained at a constant 37.0°C using a Julabo heating circulator (Julabo USA Inc, Allentown, PA, USA).

Stent-Grafts

A 180-mm Nellix system was deployed in all setups. The balloon-expandable endograft system consisted of 2 parallel 10-mm-diameter cobalt chromium alloy stent frames surrounded by expanded polytetrafluoroethylene (ePTFE) graft material. An endobag made of an inner polyester sleeve with a covered polyurethane film was attached to each stent frame proximally and distally with polyethylene sutures. The proximal attachment site was 5 mm below the uncovered "crown" on the stent frame. The endobags were filled with freshly thawed aqueous polyethylene glycol–based solutions designed to cure within 5 minutes to form a solid biostable polymer. By design the endobag unfolded in a tapered shape, so endobag sealing to the aortic wall began 5 mm distal to the stent-graft crown (Figure 2).

EVAS systems were used in 4 consecutive experiments involving 2 different types of CGs: balloon-expandable (BECG) and self-expanding (SECG). Two identical CGs were placed bilaterally in the renal branches in all experiments. In the first 2 experiments, four 6×59-mm, balloon-expandable Atrium Advanta V12 stent-grafts (Atrium
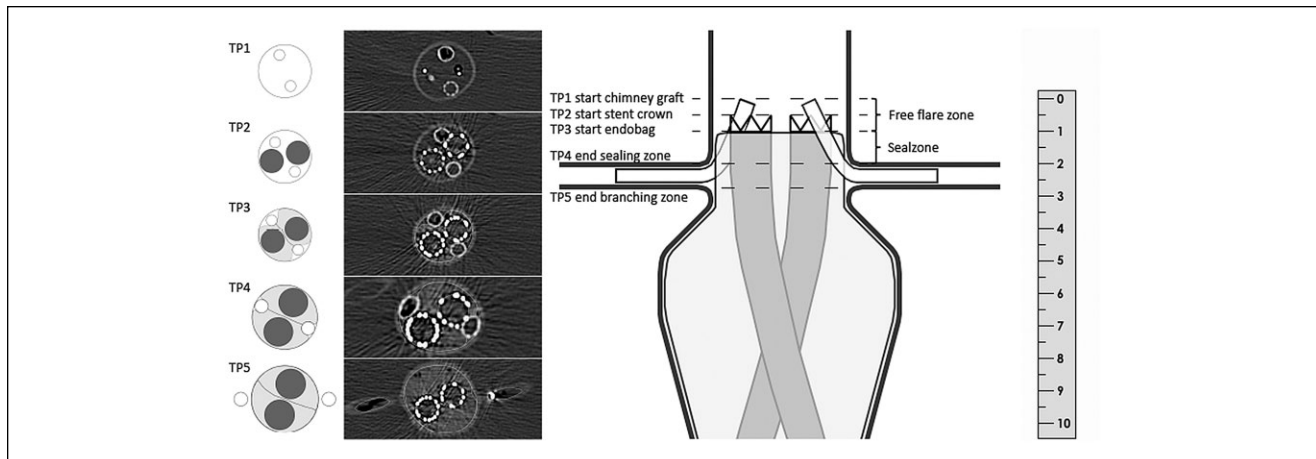
Figure 2. A longitudinal cross-section of the chimney endovascular aneurysm sealing configuration. The different table points at the start and end of the zones of interest are numbered TP1-TP5. The cross-sectional lumen areas are presented with the corresponding table positions. The aortic lumen and chimney graft lumen are in white, the endobags are in gray, and the main graft lumen is in black. The ruler is in centimeters.

Maquet Getinge Group, Mijdrecht, the Netherlands) were used. For the next 2 experiments, the chEVAS devices were removed and a new Nellix system was deployed. Four 6×50-mm self-expanding Viabahn stent-grafts (W.L. Gore & Associates, Flagstaff, AZ, USA) were employed as CGs.

Deployment

The CGs were inserted over guidewires through the suprarenal aorta in the renal branches prior to insertion of the Nellix device, which was delivered through the iliac branches. The endobags unfold 5 mm after the proximal uncovered stent crown to ensure a free-flare zone of 10 mm (Figure 2). Using a ruler under direct vision, the CGs were positioned 5 mm proximal to the stent crowns of the main endografts, which were placed 15 mm proximal to the renal branches for a 15-mm seal zone to ensure adequate sealing (Figure 2). With the delivery balloons inflated in all CGs and Nellix endografts under a constant pressure of 8 bars to prevent compression, the endobags were filled with heparinized saline (prefill) at a constant pressure of 180 mm Hg per the Nellix instructions for use. The saline was aspirated to calculate the volume for the primary fill.

With all balloons reinflated, the primary infusion of the polymer was divided in multiple stages to allow the pressure to drop below 180 mm Hg after infusion of every polymer cartridge. The delivery line was removed from the catheter after primary fill to enable secondary fill of the endobag, which took place under the same filling pressure after the primary fill cured. In the experiments involving the self-expanding CGs, 6×59-mm Advanta V12 balloons were reused and inflated following the same protocol.

Measurements

Polymer volumes (prefill, primary fill, and secondary fill) and procedure time (stent alignment time, renal ischemia time, and polymer curing time) were recorded. A 64-slice computed tomography (CT) scanner (Philips Medical Systems, Eindhoven, the Netherlands) was used to scan the entire setup after curing of each polymer fill. The geometrical analysis was performed using Osirix postprocessing software (Pixmeo, Geneva, Switzerland) as in previous in vitro studies.[10,17,18] Cross-sectional lumen areas of the CGs, main endografts, endobags, and gutters were measured after the primary fill and after the secondary fill to determine differences using 2-mm CT intervals. The areas of interest (Figure 2) were the free-flare zone from the proximal end of the CG (TP1) to the start of the covered stent (TP2), the composite sealing zone from the start of the endobag (TP3) to the top of the branch arteries (TP4), the branch zone from the top (TP4) to the bottom (TP5) of the branch arteries, and the translational zone from the distal side (TP5) of the branch arteries. Gutter surface areas were determined at the start and end of all zones of interest.

Gutter surface areas were measured perpendicular to the main endograft on a slice-to-slice basis (Figure 3A). A 3-dimensional (3D) volume of the gutter was computed from the start of the endobag to the end of the gutter using these stacked slices. Paragraft gutter volumes were measured individually (ventral and dorsal to both CGs). Likewise, a 3D volume was computed from start to end of the endobags to determine the total endobag volume. To examine a potential reduction of the sealing zone as a consequence of drooping shoulders as described by van Noort et al,[19] the craniocaudal lengths were measured of all setups in which drooping shoulders were present.
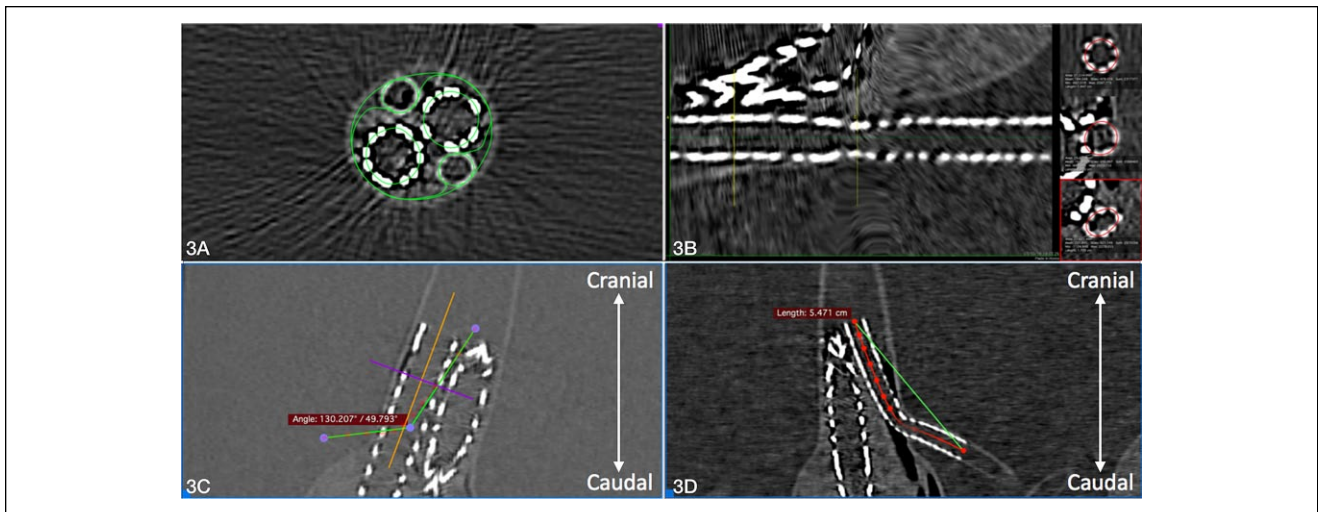
Figure 3. This image depicts the different measurements performed using Osirix postprocessing software. (A) The cross-sectional area measurement of the sealing zone in 2 different axes used for volumetric analysis of the gutters, main grafts, and endobags. (B) Perpendicular lumen area measurement for analysis of chimney graft compression. The minimum and maximum chimney graft compression, based on a central lumen line (red), is displayed. (C) The chimney graft angulation measurement based on the central lumen line. (D) The tortuosity measurement based on the central lumen line between the start and end of the chimney graft.

CG compression was measured perpendicular to central lumen lines (CLLs) created through the CGs with the built-in 3D Curved-MPR function in Osirix (Figure 3B). The surface lumen area loss per CG was calculated by subtracting the minimum CG surface lumen area at the point of maximum compression from the maximum CG surface lumen area. CG compression was expressed in percent as the CG lumen area loss (maximum CG lumen area minus the minimum CG lumen area) divided by the maximum CG lumen area after primary fill. CG angulation was measured in 3 axes (anterior-posterior, lateral, and craniocaudal). The maximum angle based on the CLL was used for comparison.

To predict disturbance in lumen circulatory flow, CG kinking was determined by measuring the degree of CG angulation between the origin and insertion of the CG in a view perpendicular to the main endograft (Figure 3C). To determine tortuosity of the CGs (Figure 3D), the distance along the CLL and absolute distance between the CG start and end were measured. Tortuosity was expressed as a ratio of the CLL length divided by the absolute length between the CG start and end.[20]

Analysis

The feasibility and optimal configuration of the different CGs in chEVAS setups were determined based on CG compression, angulation, and gutter volumes derived from the geometrical analysis. Maximum paragraft gutter areas and volumes were calculated per CG configuration (BECG and SECG) per model (19 and 24 mm) after the primary and secondary fills, as were maximum CG compression,

angulation, and tortuosity. Small sample sizes prevented statistical analysis.

Measurements were performed in duplicate by 2 independent analysts and averaged. Interobserver reproducibility of gutter measurements was assessed based on 20 randomly selected slices that were used in the computation of 3D gutter volume. The intraclass coefficient index was applied to assess reproducibility of gutter areas, gutter volume, and CG compression measurements. Values <0.40 indicated poor agreement, while fair agreement was between 0.40 and 0.59, good agreement between 0.60 and 0.74, and excellent agreement ≥0.75.[21] The analyses were performed with SPSS software (version 24.0.0.0; IBM Corporation, Armonk, NY, USA).

Results

Deployment

The Nellix EVAS systems in combination with the CGs were satisfactorily positioned and the endobags filled in all setups; 1 balloon in a Viabahn SECG (19-mm model) burst during secondary fill. Procedure time, renal ischemia time, and infused polymer volumes are displayed in Table 1. Renal ischemia times ranged from 11.5 to 12.8 minutes. Secondary fill times were 2 to 3 times longer than the primary fill.

Gutter Areas

Paragraft gutters had a conical shape and appeared to be larger at the proximal end of the seal zone (Figure 2 and

Table 1. Procedure Times for the 2 Suprarenal Aortic Diameter Models According to the Type of Chimney Graft Deployed.[a]

Time	Advanta Chimney Graft		Viabahn Chimney Graft	
	19-mm Model	24-mm Model	19-mm Model	24-mm Model
Total experiment	18:22	22:59	17:14	14:55
Primary fill	3:30	2:50	2:10	2:30
Secondary fill	6:58	9:18	6:50	5:35
Renal ischemia[b]	12:29	11:31	12:50	12:20
Curing	6:07	6:37	6:19	5:38

[a]Times given in minutes:seconds.
[b]Average of left and right renal branches.

Supplementary Figure 1, which is available in the online version of the article). The individual gutter areas after primary and secondary fills are presented in Table 2. After primary fill, the maximum gutter areas at the proximal end of the endobag (TP3) were 17.5 and 17.8 mm^2 when using the BECG and 11.0 and 17.5 mm^2 when using the SECG in the 19- and 24-mm models, respectively. At the end of the sealing zone (TP4) the maximum gutter areas were 6.1 and 9.6 mm^2 when using the BECG but slightly smaller when using the SECG (5.3 and 7.2 mm^2). At the distal branch zone (TP5) the maximum gutter areas were 3.6 and 4.2 mm^2 when using the BECG vs 5.7 and 3.9 mm^2 when using the SECG.

After secondary fill, the maximum gutter areas in the model at the proximal end of the endobag (TP3) reduced to 10.7 and 15.4 mm^2 when using the BECG and to 9.5 and 15.3 mm^2 when using the SECG in the 19- and 24-mm models, respectively (Table 2). At the end of the sealing zone (TP4) the maximum gutter areas reduced to 4.5 and 5.5 mm^2 when using the BECG and to 3.9 and 5.5 mm^2 when using the SECG. At the distal branch zone (TP5) the maximum gutter areas reduced to 2.4 and 2.2 mm^2 when using the BECG and to 5.0 and 2.0 mm^2 when using the SECG. Lumen gutter areas appeared to be larger in the models with a wider aneurysm neck, while no differences were found in paragraft gutter lumen areas between the BECG and SECG.

Gutter Volumes

In all the digitally created 3D models, the paragraft gutters had similar tapered shapes, which coincided with the larger dimensions in the proximal seal zone and smaller values toward the distal end of the seal zone (Table 2). According to the gutter classification of Overeem et al,[8] the gutters were categorized as type A3 (from proximal CG configuration to proximal of the aneurysm) and slightly more distal type A1 (from proximal CG configuration to proximally within the aneurysm). No gutters were found within the renal branches.

The maximum gutter volumes (Figure 4A) after primary fill were 84.2 and 99.4 mm^3 when using the BECG and 67.2 and 92.7 mm^3 when using the SECG in the 19- and 24-mm models, respectively. After secondary fill the gutter volumes reduced to 73.1 mm^3 (13.2% change) and 72.0 mm^3 (27.6% change) when using the BECG, whereas gutter volumes reduced to 44.0 mm^3 (34.5% change) and 82.3 mm^3 (11.2% change) when using the SECG.

Endobag Volumes

The total endobag volumes (Table 2) after primary fill were 151.8 and 152.6 cm^3 when using the BECG and 152.7 and 157.1 cm^3 when using the SECG in the 19- and 24-mm models, respectively. Secondary fill of the endobags appeared to increase endobag volumes in all setups. After secondary fill the endobag volume increased to 161.6 cm^3 (6.4%) and 162.4 cm^3 (6.4%) when using the BECG vs 164.5 cm^3 (7.7%) and 166.1 cm^3 (5.7%) when using the SECG in the 19- and 24-mm models, respectively.

Drooping Shoulders

Examination of the craniocaudal length of drooping shoulders of the endobags revealed a mean length of 1.0 mm (range 0.8–1.4), resulting in a 10% decrease of sealing zone length.
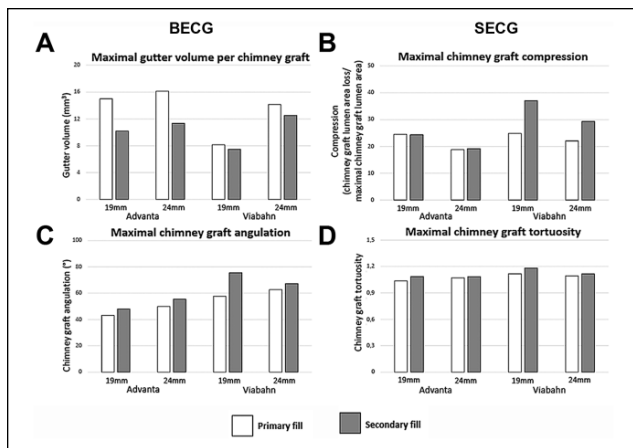
CG Compression

Analysis showed CG compression in all setups after primary fill (Figure 4B). Secondary fill increased CG compression in most configurations except a BECG in the 19-mm model and another BECG in the 24-mm model (Table 2). After primary fill BECG compression was 24.5% and 17.8% in the left renal branch and 14.0% and 18.8% in the right renal branch in the 19- and 24-mm models, respectively. SECG compression was 24.8% and 22.0% in the left renal branch and 21.1% and 17.8% in the right renal branch. After secondary fill BECG compression changed to 24.3%

Table 2. Postprocedural Measurements of All Suprarenal Aortic Diameter Models According to the Type of Chimney Graft Deployed.

| | Advanta CG | | | | | | Viabahn CG | | | | | |
| | 19-mm Model | | | 24-mm Model | | | 19-mm Model | | | 24-mm Model | | |
Variable	Primary Fill	Secondary Fill	Change, %	Primary Fill	Secondary Fill	Change, %	Primary Fill	Secondary Fill	Change, %	Primary Fill	Secondary Fill	Change, %
Polymer volume, cm^3	140	10	7.1	153	9	5.9	145	13	9.1	145	18	12.4
Endobag volume, cm^3	151.8	161.6	6.4	152.6	162.4	6.4	152.7	164.5	7.7	157.1	166.1	5.7
Gutter areas, mm^2												
TP3 proximal seal zone												
LRA ventral	17.5	10.7	38.8	17.8	14.4	18.8	9.8	9.5	3.0	17.5	15.3	12.3
LRA dorsal	5.2	4.0	24.3	16.1	15.4	4.0	5.3	4.9	6.9	14.0	13.2	5.8
RRA ventral	12.8	4.9	61.6	15.9	13.6	14.4	6.6	4.8	26.4	14.8	8.8	40.6
RRA dorsal	7.3	6.9	3.8	5.6	5.4	3.8	11.0	8.2	25.4	11.8	9.8	16.3
TP4 distal seal zone												
LRA ventral	6.1	4.4	28.4	5.8	4.8	16.6	4.8	3.9	19.5	4.1	4.9	−18.6
LRA dorsal	5.9	2.7	54.4	9.6	3.6	62.6	2.5	1.7	32.9	7.2	5.5	23.5
RRA ventral	4.6	2.1	53.8	6.2	3.5	43.6	2.1	1.8	14.8	6.5	3.4	46.6
RRA dorsal	4.8	4.5	5.3	6.7	5.5	18.1	5.3	3.5	33.9	5.1	4.4	13.9
TP5 distal branching zone												
LRA ventral	2.3	2.2	5.1	2.9	2.2	25.6	3.1	1.6	46.1	3.1	1.8	52.9
LRA dorsal	2.8	1.2	57.9	2.9	2.0	31.6	3.3	2.1	36.5	3.2	2.0	37.3
RRA ventral	3.6	1.6	54.6	4.2	2.1	50.8	4.3	2.7	38.1	3.6	1.2	66.9
RRA dorsal	3.1	2.4	22.3	3.2	2.0	37.4	5.7	5.0	13.5	3.0	1.3	55.8
Gutter volume, mm^3												
LRA ventral	84.0	35.4	57.9	99.4	72.0	27.6	45.1	44.0	2.4	59.7	54.5	8.7
LRA dorsal	76.9	65.0	15.5	51.0	32.5	36.3	45.8	43.5	5.0	92.7	82.3	11.2
RRA ventral	54.7	30.3	44.6	87.9	53.1	39.6	25.1	21.2	15.5	50.9	39.1	23.2
RRA dorsal	84.2	73.1	13.2	84.3	69.4	17.7	67.2	40.7	13.8	79.3	74.6	5.9
CG compression, %												
LRA	24.5	24.3	−0.2	17.8	16.8	−1.0	24.8	35.0	10.2	22.0	29.3	7.2
RRA	14.0	19.4	5.4	18.8	19.1	0.4	21.1	37.1	16.0	17.8	25.1	7.3
CG angulation, deg												
LRA	43.1	48.0	11.4	45.6	50.0	9.6	57.7	70.1	21.5	52.3	67.3	28.7
RRA	31.3	42.8	36.7	49.9	55.4	11.0	51.2	75.5	47.5	62.7	66.5	6.1
CG tortuosity												
LRA	1.03	1.09	5.5	1.07	1.09	1.3	1.12	1.17	5.0	1.05	1.08	1.9
RRA	1.04	1.08	3.7	1.07	1.08	1.3	1.09	1.18	8.5	1.10	1.12	1.9

Abbreviations: CG, chimney graft; LRA, left renal artery; RRA, right renal artery.

Figure 4. (A) The average gutter volume, (B) chimney graft compression, (C) chimney graft angulation, and (D) chimney graft tortuosity per model in white after the primary fill and in gray after the secondary fill for both the Advanta balloon-expandable chimney grafts (BECG) and the Viabahn self-expanding chimney grafts (SECG).

and 16.8% in the left branch and to 19.4% and 19.1% in the right. SECG compression changed to 35.0% and 29.3% in the left branch and to 37.1% and 25.1% in the right. The highest change of CG compression within the same individual CG was 5.4% and 0.4% for the BECG and 16.0% and 7.3% for the SECG in the 19- and 24-mm models, respectively. The largest increase in CG compression was found in the SECG with the burst balloon (19-mm model).

CG Angulation

The CG angulation increased after the secondary fill of the endobags in all setups (Table 2). After primary fill, the maximum angulations were 43.1° and 49.9° when using the BECG vs 57.7° and 62.7° when using the SECG in the 19- and 24-mm models, respectively. After secondary fill, the average angulations were 48.0° (11.4% change) and 55.4° (11.0% change) when using the BECG and 75.5° (30.8%) and 67.3° (7.3%) when using the SECG (Figure 4C). The highest CG angulation was in the SECG in which the balloon burst.

CG Tortuosity

Tortuosity increased in all CGs after secondary fill of the endobags corresponding to changes in CG angulation (Table 2). After primary fill, maximum tortuosity ratios were 1.04 and 1.07 when using the BECG vs 1.12 and 1.10 when using the SECG in the 19- and 24-mm models, respectively. After secondary fill, the average tortuosity ratios were 1.09 (4.8% change) and 1.09 (1.3% change) when using the BECG vs 1.18 (5.8% change) and 1.12 (1.9%

change) when using the SECG (Figure 4D). The highest CG tortuosity was found in the SECG in which the balloon burst.

Measurement Reproducibility

Measurements of gutter volumes and CG compression showed acceptable reproducibility. The intraclass correlation coefficient for volume measurements was 0.725 (good agreement), while the interclass correlation for compression measurements was 0.784 (excellent agreement).

Discussion

Based on these experiments, secondary fill reduced gutter volumes in all setups but did not obliterate the gutters. This partial reduction of gutters was, however, associated with increased CG compression in 6 of 8 CGs despite inflating balloons in all stent-grafts during both primary and secondary fills. During the last experiment, a balloon burst in one SECG in the 19-mm model during secondary fill; the reused Advanta balloon might have been damaged on earlier extraction. This configuration had the highest CG compression and tortuosity, presumably due to the balloon malfunction.

Tortuosity and angulation of the CGs increased after secondary fill in all setups. In our model, neither were renal branches connected to end organs nor was there resistance around the aneurysm that would have been provided by surrounding retroperitoneal structures, which may have contributed to the greater angulation in both CGs. The larger total values in both angulation and tortuosity in the SECG compared with the BECG may have been caused by the burst balloon. Moreover, a slightly larger volume of polymer was infused during secondary fill when using the SECG compared to the BECG. Furthermore, CG compression decreased slightly in the left renal branch of the BECG in both models, perhaps because of (temporarily higher) inflation pressure than specified in the instructions for use.

Previous studies evaluating chEVAS configurations suggested that conformation of endobags around the CGs could reduce or obliterate formation of paragraft gutters.[22–24] However, our previous publication[17] showed that in vitro chEVAS configurations could still contain small paragraft gutters, later confirmed by Boersen et al.[25] The current experiments confirmed the presence of paragraft gutters in chEVAS configurations in vitro after primary fill, and although secondary fill reduced gutter size, these paragraft gutters were not eradicated. Since it is not possible to distinguish the polymer injected during primary and secondary fill postprocedurally, the exact location of the secondary fill polymer could not be determined. The clinical advantage of reducing gutter size without completely obliterating the gutter is unknown insofar as endoleaks are concerned.

However, whether or not these findings translate into clinical significance requires further study.

Increased CG compression is a detrimental effect that might be augmented by polymer infusion during both primary and secondary fills in a nonanatomical space as a consequence of CG straightening by the balloon. The primary fill forms an irreversible polymer cast after curing; the secondary fill narrows the polymer cast. Deflation of the balloons relocates the renal branches and CGs at least partly in the initial configuration. This relocation into the narrowed polymer cast conceivably leads to the seemingly increased CG compression. It is therefore possible that adequate balloon inflation during the procedure does not prevent CG compression after secondary fill. This additional endobag filling conjointly prolonged renal ischemia time and should be used with caution. However, compared to open repair requiring suprarenal clamping,[26] the renal ischemia times are still relatively short. Clinical significance of this ischemia time could not be determined and requires further study.

The polymer volume delivered through both catheters during secondary fill (average 12.5 mL of polymer) seems large even though the primary fill was considered adequate at 180 mm Hg. However, during clinical deployment the pressure is sometimes raised above 180 mm Hg.[23,27] The compliance of the silicone aneurysm and the absence of surrounding retroperitoneal pressure may have allowed the use of a larger volume without raising the filling pressure. Also, secondary fill seemed to reduce all paragraft gutters. It is assumed that the polymer used in secondary fill spread throughout the entire aneurysm and aneurysm neck to form a polymer cast in a nonanatomical configuration. Therefore, a relatively large volume could be infused during secondary fill without exceeding the maximum infusion pressure (180 mm Hg) advised by the manufacturers.

The aneurysm neck in the silicone models was designed to mimic that of the healthy human aorta. Compliance depends on the wall thickness and lumen diameter and therefore varies throughout the aneurysm, especially in the stiffer renal arteries. In our model, the stiffness of the renal branches might have been counterbalanced by the lack of physiological resistance normally provided by the surrounding tissue and kidneys. These silicone walls have a more linear mechanical aspect than actual vascular tissues and do not completely represent pathological variabilities of the vascular wall yet accommodate sufficient sealing of the endobags. Similar silicone models proved an established and valuable testing methodology in academic and medical device industry research. Furthermore, the absence of distal fixation of the renal branches could have led to their increased movement during deployment of the renal stent-grafts, possibly influencing the final position and gutter size. For the hypothesis tested in this study, comparing the effect of primary and secondary filling on gutter sizes, the models are considered acceptable.[28–30] However, a note of caution is due here since these models are only a simplified version of the in vivo situation. One should bear in mind that many factors concerning anatomy, physiology, and pathology not considered in the current study might influence chEVAS deployment success. Furthermore, with a small sample size, caution must be applied; differences were not tested for statistical significance.

According to Overeem et al,[8] not all paragraft gutters cause a type Ia endoleak.[8] Small paragraft gutters do not influence successful endovascular repair, since they are occluded by progressive thrombus formation during early follow-up.[5,25] In addition, de Beaufort et al[31] describe a reduction of gutter sizes in CG configurations during follow-up. Hence, most perioperative type Ia endoleaks do not persist during midterm follow-up.[5,8,25,31] However, Niepoth et al[17] state that these paragraft gutters might increase or decrease based on vascular wall movements and through the force of blood pressure on the proximal sealing zone, which could lead to aneurysm growth and the need for secondary interventions. It should be noted, though, that the geometrical changes in paragraft gutters observed in our static models in a gelatin-water environment were not tested for the influence of pressure or spontaneous thrombosis of these gutters. Therefore, the correlation of paragraft gutter reduction and the occurrence of type Ia endoleak and aneurysm rupture has to be determined in future studies.

Despite the occurrence of endoleaks, CG configurations provide a minimally invasive and cost-effective approach, which is available in emergent settings since off-the-shelf stent-grafts are used. In an attempt to optimize CG configurations and reduce these gutters, clinicians have used a combination of EVAS systems with CGs to reduce gutter sizes by filling the endobags.[11,12,17,32] Recently, Stenson et al[33] described a single-center experience with the use of the chEVAS in complex aortic aneurysms. The authors suggested that this configuration is a potential solution, especially in elderly patients with multiple comorbidities.

A general note on sealing zone calculation in EVAS should be provided in accord with a previous study published by van Noort et al.[19] In our setups, a mean 10% decrease of sealing zone was found as a consequence of drooping shoulders. Therefore, this event should be considered in endobag sealing zone calculations. The first publications describing EVAS safety and efficacy showed adequate outcomes[11,34,35]; however, long-term device limitations, migration, and sac remodeling have to be studied more closely to prove whether this technique is a feasible and effective approach.[36,37]

Conclusion

In this study, secondary endobag filling using balloon-expandable and self-expanding CGs in chEVAS configurations reduced the paragraft gutter volume but did not

obliterate the gutters. Meanwhile, secondary endobag filling could come at the expense of increased CG compression and prolonged renal ischemia time.

ORCID iD

Theodorus G. van Schaik (iD) https://orcid.org/0000-0002-1160-1085

References

1. Jongkind V, Yeung KK, Akkersdijk GJ, et al. Juxtarenal aortic aneurysm repair. *J Vasc Surg*. 2010;52(3):760–767.
2. Rao R, Lane TR, Franklin IJ, et al. Open repair versus fenestrated endovascular aneurysm repair of juxtarenal aneurysms. *J Vasc Surg*. 2015;61:242–255.
3. Coscas R, Kobeiter H, Desgranges P, et al. Technical aspects, current indications, and results of chimney grafts for juxtarenal aortic aneurysms. *J Vasc Surg*. 2011;53:1520–1527.
4. Lindblad B, Bin Jabr A, Holst J, et al. Chimney grafts in aortic stent grafting: hazardous or useful technique? systematic review of current data. *Eur J Vasc Endovasc Surg*. 2015;50:722–731.
5. Ullery BW, Tran K, Itoga NK, et al. Natural history of gutter-related type Ia endoleaks after snorkel/chimney endovascular aneurysm repair. *J Vasc Surg*. 2017;65:981–990.
6. Donas KP, Lee JT, Lachat M, et al; PERICLES Investigators. Collected world experience about the performance of the snorkel/chimney endovascular technique in the treatment of complex aortic pathologies: the PERICLES registry. *Ann Surg*. 2015;262:546–553.
7. Wilson A, Zhou S, Bachoo P, et al. Systematic review of chimney and periscope grafts for endovascular aneurysm repair. *Br J Surg*. 2013;100:1557–1564.

8. Overeem SP, Boersen JT, Schuurmann RCL, et al. Classification of gutter type in parallel stenting during endovascular aortic aneurysm repair. *J Vasc Surg*. 2017;66:594–599.
9. Donselaar EJ, Holden A, Zoethout AC, et al. Feasibility and technical aspects of proximal Nellix-in-Nellix extension for late caudal endograft migration. *J Endovasc Ther*. 2017;24:210–217.
10. de Bruin JL, Yeung KK, Niepoth WW, et al. Geometric study of various chimney graft configurations in an in vitro juxtarenal aneurysm model. *J Endovasc Ther*. 2013;20:184–190.
11. Batagini NC, Hardy D, Clair DG, et al. Nellix EndoVascular Aneurysm Sealing System: device description, technique of implantation, and literature review. *Semin Vasc Surg*. 2016;29:55–60.
12. Rouer M, El Batti S, Julia P, et al. Chimney stent graft for endovascular sealing of a pararenal aortic aneurysm. *Ann Vasc Surg*. 2014;28:1936.e15–1936.e18.
13. Brownrigg JR, de Bruin JL, Rossi L, et al. Endovascular aneurysm sealing for infrarenal abdominal aortic aneurysms: 30-day outcomes of 105 patients in a single centre. *Eur J Vasc Endovasc Surg*. 2015;50:157–164.
14. Gossetti B, Martinelli O, Ferri M, et al; IRENE Group Investigators. Preliminary results of endovascular aneurysm sealing from the multicenter Italian Research on Nellix Endoprosthesis (IRENE) study. *J Vasc Surg*. 2018;67:1397–1403.
15. Mahmoodani F, Ardekani VS, See SF, et al. Optimization and physical properties of gelatin extracted from pangasius catfish (*Pangasius sutchi*) bone. *J Food Sci Technol*. 2014;51:3104–3113.
16. Yousif MY, Holdsworth DW, Poepping TL. Deriving a blood-mimicking fluid for particle image velocimetry in Sylgard-184 vascular models. *Conf Proc IEEE Eng Med Biol Soc*. 2009;2009:1412–1415.
17. Niepoth WW, de Bruin JL, Lely RL, et al. In vitro feasibility of a sac-sealing endoprosthesis in a double chimney graft configuration for juxtarenal aneurysm. *J Endovasc Ther*. 2014;21:529–537.
18. Niepoth WW, de Bruin JL, Yeung KK, et al. A proof-of-concept in vitro study to determine if EndoAnchors can reduce gutter size in chimney graft configurations. *J Endovasc Ther*. 2013;20:498–505.
19. van Noort K, Overeem SP, van Veen R, et al. Apposition and positioning of the Nellix EndoVascular Aneurysm Sealing System in the infrarenal aortic neck. *J Endovasc Ther*. 2018;25:428–434.
20. Ghatwary T, Karthikesalingam A, Patterson B, et al. St George's Vascular Institute Protocol: an accurate and reproducible methodology to enable comprehensive characterization of infrarenal abdominal aortic aneurysm morphology in clinical and research applications. *J Endovasc Ther*. 2012;19:400–414.
21. Cicchetti DV. Guidelines, criteria, and rules of thumb for evaluating normed and standardized assessment instruments in psychology. *Psychological Assessment*. 1994;6:284–290.
22. Dijkstra ML, Lardenoye JW, van Oostayen JA, et al. Endovascular aneurysm sealing for juxtarenal aneurysm using the Nellix device and chimney covered stents. *J Endovasc Ther*. 2014;21:541–547.

23. Malkawi AH, de Bruin JL, Loftus IM, et al. Treatment of a juxtarenal aneurysm with the Nellix endovascular aneurysm sealing system and chimney stent. *J Endovasc Ther*. 2014;21:538–540.

24. Torella F, Chan TY, Shaikh U, et al. ChEVAS: Combining suprarenal EVAS with chimney technique. *Cardiovasc Intervent Radiol*. 2015;38:1294–1298.

25. Boersen JT, Donselaar EJ, Groot Jebbink E, et al. Benchtop quantification of gutter formation and compression of chimney stent grafts in relation to renal flow in chimney endovascular aneurysm repair and endovascular aneurysm sealing configurations. *J Vasc Surg*. 2017;66:1565–1573.e1.

26. Knott AW, Kalra M, Duncan AA, et al. Open repair of juxtarenal aortic aneurysms (JAA) remains a safe option in the era of fenestrated endografts. *J Vasc Surg*. 2008;47:695–701.

27. Boersen JT, van den Ham LH, Heyligers JM, et al. Validation of pre-procedural aortic aneurysm volume calculations to estimate procedural fill volume of endobags in endovascular aortic sealing. *J Cardiovasc Surg (Torino)*. 2017;58:674–679.

28. Abel DB, Dehdashtian MM, Rodger ST, et al. Evolution and future of preclinical testing for endovascular grafts. *J Endovasc Ther*. 2006;13:649–659.

29. Ohta M, Handa A, Iwata H, et al. Poly-vinyl alcohol hydrogel vascular models for in vitro aneurysm simulations: the key to low friction surfaces. *Technol Health Care*. 2004;12:225–233.

30. Sulaiman A, Boussel L, Taconnet F, et al. In vitro non-rigid life-size model of aortic arch aneurysm for endovascular prosthesis assessment. *Eur J Cardiothorac Surg*. 2008;33:53–57.

31. de Beaufort HWL, Cellitti E, de Ruiter QMB, et al. Midterm outcomes and evolution of gutter area after endovascular aneurysm repair with the chimney graft procedure. *J Vasc Surg*. 2018;67:104–112.e3.

32. De Bruin JL, Brownrigg JR, Patterson BO, et al. The endovascular sealing device in combination with parallel grafts for treatment of juxta/suprarenal abdominal aortic aneurysms: short-term results of a novel alternative. *Eur J Vasc Endovasc Surg*. 2016;52:458–465.

33. Stenson KM, De Bruin JL, Holt PJ, et al. Extended use of endovascular aneurysm sealing: chimneys for juxtarenal aneurysms. *Semin Vasc Surg*. 2016;29:120–125.

34. Kostun ZW, Woo EY. Endovascular aneurysm sealing addresses several limitations of conventional endovascular aneurysm repair. *Semin Vasc Surg*. 2016;29:50–54.

35. Holden A. Clinical outcomes after Nellix Endovascular Aneurysm Sealing. *Semin Vasc Surg*. 2016;29:102–105.

36. Reijnen MMPJ, Holden A. Status of endovascular aneurysm sealing after 5 years of commercial use. *J Endovasc Ther*. 2018;25:201–206.

37. van Noort K, Boersen JT, Zoethout AC, et al; DEVASS Dutch Endovascular Aneurysm Sealing Study Group. Anatomical predictors of endoleaks or migration after endovascular aneurysm sealing. *J Endovasc Ther*. 2018;25:719–725.